PL-TR--93-1058

PL-TR--
93-1058

PHASE-ONLY CORRECTION OF SCINTILLATED LASER BEAMS: DOWNRANGE EXPERIMENTAL RESULTS

(2)

L. McMackin et al.

March 1994

Final Report

PHILLIPS LABORATORY
LASERS AND IMAGING DIRECTORATE
AIR FORCE MATERIEL COMMAND
KIRTLAND AIR FORCE BASE, NM 87117-5776

REPORT DOCUMENTATION PAGE

Form Approved
OMB No. 0704-0188

1. AGENCY USE ONLY *(Leave blank)*	2. REPORT DATE	3. REPORT TYPE AND DATES COVERED
	March 1994	Final

4. TITLE AND SUBTITLE
PHASE-ONLY CORRECTION OF SCINTILLATED LASER BEAMS: DOWNRANGE EXPERIMENTAL RESULTS

5. FUNDING NUMBERS
PR: 9993
TA: LA
WU: BS

6. AUTHOR(S)
McMackin, L., Gonglewski, J.D., Venet, B., Jelonek, M.P., *Spinherne, J.M., Dymale, R.C., **Bishop, K.P., and ***Oliker, M.

7. PERFORMING ORGANIZATION NAME(S) AND ADDRESS(ES)
Phillips Laboratory
3550 Aberdeen Avenue SE
Kirtland AFB, NM 87117-5776

8. PERFORMING ORGANIZATION REPORT NUMBER
PL-TR--93-1058

9. SPONSORING / MONITORING AGENCY NAME(S) AND ADDRESS(ES)

10. SPONSORING / MONITORING AGENCY REPORT NUMBER

11. SUPPLEMENTARY NOTES
Publication of this report does not constitute approval or disapproval of the ideas or findings. It is published in the interest of scientific and technical exchange. The established procedures for editing reports were not followed for this technical report.

12a. DISTRIBUTION / AVAILABILITY STATEMENT
Approved for public release; distribution is unlimited.

12b. DISTRIBUTION CODE

13. ABSTRACT *(Maximum 200 words)*

Results of a Horizontal Propagation Experiment (HoPe) that was performed at the Phillips Laboratory Starfire Optical Range are presented. In this experiment, a laser beam was phase corrected using an adaptive optics system located at the transmitting site and focused toward a target located two miles away. Irradiance patterns of the corrected and uncorrected beam were recorded at the target site. Weather and atmospheric turbulence characteristics along the optical path were recorded at the same time. Strehl ratios calculated from the recorded images show that phase-only correction of a horizontally propagated laser beam can significantly improve the energy collected on-axis even under strongly scintillated conditions. Time-averaged Strehl ratios were improved by as much as a factor of five. Improvements in strehl for varying turbulence conditions and the effect of hardware limitations on the results are discussed.

*Rockwell Power Systems, Albuquerque, NM
**Applied Technology Associates, Albuquerque, NM
***Adaptive Optics associates, Albuquerque, NM

14. SUBJECT TERMS	15. NUMBER OF PAGES
Wavefront Sensing, Phase-only Correction, Optical Scintillation, Adaptive Optics	12
	16. PRICE CODE

17. SECURITY CLASSIFICATION OF REPORT	18. SECURITY CLASSIFICATION OF THIS PAGE	19. SECURITY CLASSIFICATION OF ABSTRACT	20. LIMITATION OF ABSTRACT
Unclassified	Unclassified	Unclassified	

Phase-only correction of scintillated laser beams: downrange experimental results

Lenore McMackin, John D. Gonglewski, Boris Venet, Mark P. Jelonek
Phillips Laboratory, Kirtland AFB, NM 87117

J. M. Spinherne, Raymond C. Dymale
Rockwell Power Systems, Albuquerque, NM

K. P. Bishop
Applied Technology Associates, Albuquerque, NM

Michael Oliker
Adaptive Optics Associates, Albuquerque, NM

ABSTRACT

We present the results of a Horizontal Propagation Experiment (HoPE) that was performed at the Phillips Laboratory Starfire Optical Range. In this experiment a laser beam was phase corrected using an adaptive optics system located at the transmitting site and focused toward a target located two miles away. Irradiance patterns of the corrected and uncorrected beam were recorded at the target site. Weather and atmospheric turbulence characteristics along the optical path were recorded at the same time. Strehl ratios calculated from the recorded images show that phase-only correction of a horizontally propagated laser beam can significantly improve the energy collected on-axis even under strongly scintillated conditions. Time-averaged Strehl ratios were improved by as much as a factor of 5. Improvements in Strehl for varying turbulence conditions and the effect of hardware limitations on the results are discussed.

1. TRANSMITTER AND COMPENSATION SYSTEM

The function of the transmitting system shown simplified in Fig. 1 is to provide a focused laser beam that is compensated for phase errors incurred by atmospheric turbulence along the two mile path. A beacon laser , $\lambda = 633$ nm, originating from the center of the target impinges on a Shack-Hartmann wavefront sensor (WFS) located 2 miles from the target at the Starfire Optical Range. The sensor determines the phase of the beacon from measurements of the gradients of the wavefront over each subaperture using a least squares reconstruction algorithm. The computed phase is conjugated and imprinted onto the scoring laser beam ($\lambda = 612$ nm) using a deformable mirror consisting of a 16 x 16 array of actuated square subapertures each effectively 7 mm across in the entrance pupil. The deformable mirror also focuses the phase corrected signal beam that is then sent to the target.

Gross tilt in the wavefront (beam steering) can be dealt with in two ways in the transmitting adaptive optics system. The first is by using a steering mirror that controls the direction of the beam. The second is by using the deformable mirror to correct for both tilt and higher order aberrations. Results from both methods are described.

In addition to phase conjugation, wavefront sensor gradient data collected during operation of the experiment is used to calculate path integrated values of the atmospheric coherence parameter, r_0. The calculated r_0 is used to calculate an average value of C_n^2. The WFS data is also used to obtain path integrated values of the log amplitude variance, a measure of the amount of scintillation induced by turbulence along the 2 mile path.

2. RECEIVER DESIGN

The HoPE receiver, shown schematically in Fig. 1, is designed to capture images of the scoring laser transmitted by the Starfire Optical Range (SOR) adaptive optics system. Scoring laser light at $\lambda = 612$ nm sent from the transmitter propagates from right to left in the figure. The signal impinges on the receiver aperture consisting of a 16 inch diameter off-axis parabolic mirror (OAP) with a focal length of 100 inches. The mirror focuses the signal onto an imaging system and a

photomultiplier tube. The beacon is an unexpanded HeNe laser $\lambda = 633$ nm entering the system through beamsplitter (BS) and counterpropagating with respect to the incoming signal. The beacon allows the transmitter to track the target through turbulent jitter and is used to correct the signal phase.

A system of camera lenses images the signal (with approximate magnification of 1/55) onto a Photometrics CCD camera. The effective pixel size (on the OAP aperture) is approximately 1.5 mm. The signal to be detected is modulated by an acoustooptic modulator located at the transmitter into 100 μsec pulses at intervals of 1 second. The pulse length was chosen to "freeze" the atmosphere so that each snapshot would represent the result of instantaneous correction that could be correlated to a particular deformable mirror figure. The 1 Hz repetition rate was chosen for ease of operation of the Photometrics camera and to allow a background exposure to be taken between laser pulses. The total power of each pulse is approximately 20 μW.

Image data was collected in sets of 110 successive snapshots each containing 256 x 256 pixels. Data acquisition of each data set was triggered by a signal from the PMT at the arrival of the initial signal pulse. An image containing only background noise was taken 0.5 seconds after every signal frame giving 55 signal shots and 55 backgrounds for each data set. Recording interlaced background frames allowed the background to be subtracted from each signal frame during data reduction. Removing the background noise from the data was an important consideration for daylight operation of the experiment. Additional background removal features were also incorporated into the design as outlined below.

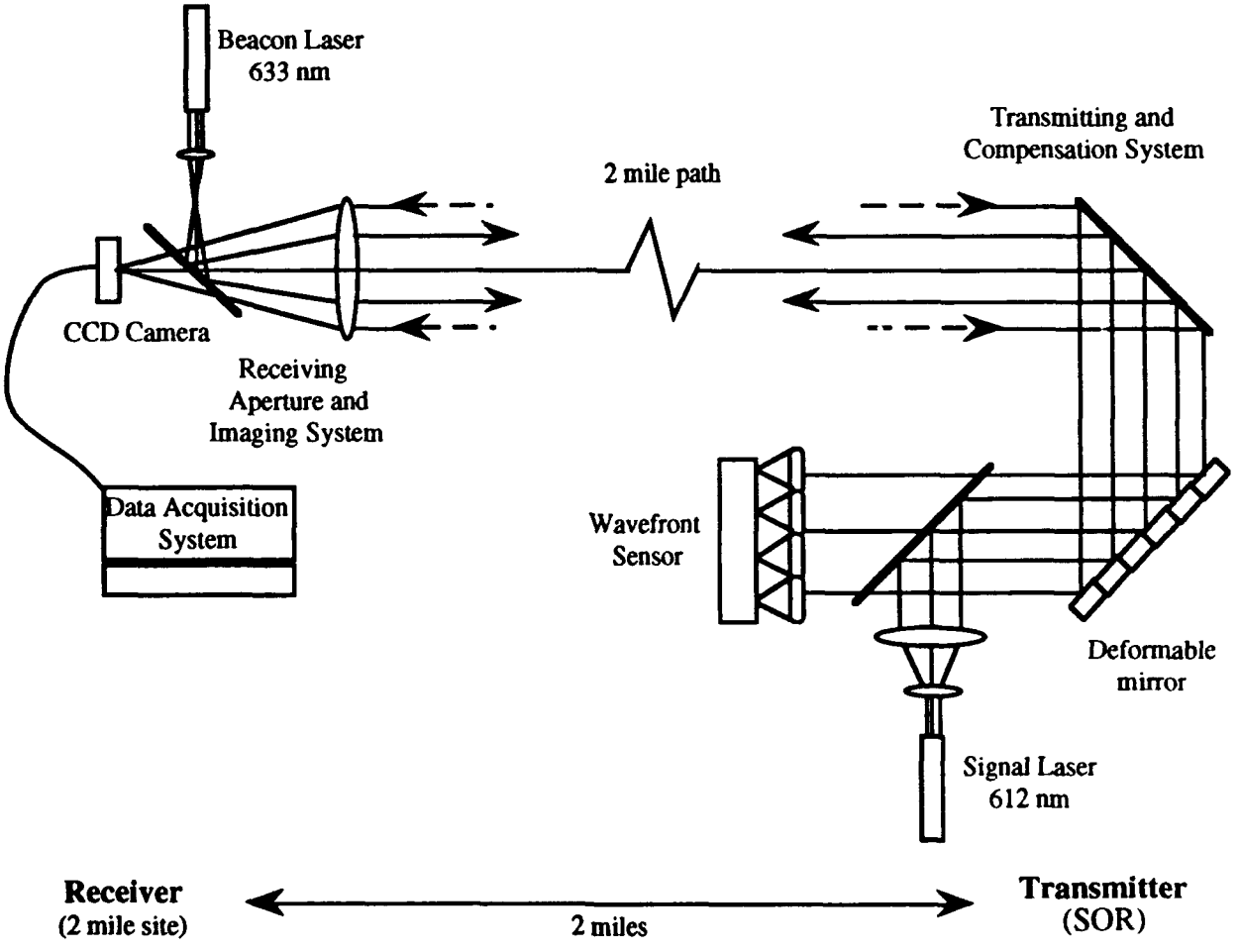

Fig. 1. Simplified transmitter and receiver schematic. The signal beam is phase compensated at the transmitter site, propagated along a two mile path, and recorded at the receiver site.

3. RECEIVER DESIGN CONSIDERATIONS

3.1. Daylight Background Removal

Atmospheric high and saturated turbulence levels required by this experiment are most likely to occur from midmorning to mid afternoon along the chosen horizontal path. Such daylight operation requires careful removal of scattered daylight background from signal images. Background attenuation was accomplished by using a narrow band spectral filter in the imaging system that rejects all but a small region of the spectrum around the 612 nm signal wavelength. In addition, a 2 mm diameter field stop was placed at the focus of the OAP to reduce the system's field of view. These two features resulted in an average signal-to-background ratio across the receiver ~ 9. Background removal was also done using computer code by subtracting recorded background frames from corresponding signal frames during reduction and analysis of the data.

3.2. Receiver Aperture Size

Precise measurements of the Strehl of the signal beam at the target require detection of all of the incident radiation. For total power P, the Strehl, S, which is the ratio of the aberrated on-axis PSF to the unaberrated Airy peak, can be calculated from the following,

$$S = \frac{I(0)}{P\left[\frac{A_p g}{(\lambda z)^2}\right]}, \qquad (1)$$

where I(0) is the measured peak intensity, A_p is the area of the transmitter pupil, λ is the wavelength (612 nm), z is the path length (3.2 km) and g is a factor ≈ 1 that accounts for the Gaussian shape of the wavefront. The diffraction limited Airy central lobe diameter which is proportional to the path length, is about 5 cm and contains approximately 80% of the total energy. The remaining energy is located outside the central lobe in rings of successively larger radius and smaller amplitude.

Uncorrected aberrations in the beam enlarge the spot size and put more energy into the outer radii of the PSF. If the beam were aberrated enough, a significant amount of energy would miss the receiver aperture, not be included in a measurement of P in Equation 1, and the accuracy of the Strehl measurement would decrease. Figure 2 shows a family of curves that depict for a given Strehl the percentage of power in the aberrated PSF that would be captured by an aperture of a given diameter. It was calculated that for aberrations leading to a Strehl of 0.05, a circular aperture with a 40 cm diameter would capture over 95% of the energy in the spot. Thus, the 16 inch diameter OAP could accurately measure uncorrected Strehls down to 0.05. Higher Strehls (with more compact spots) are measured with even higher accuracy. Strehl reductions for Fig. 2 were calculated for a circular aperture with random aberrations characterized by the uncompensated atmospheric turbulence structure function,

$$D(r_p) = 6.88\left(\frac{r_p}{r_o}\right)^{\frac{5}{3}}. \qquad (2)$$

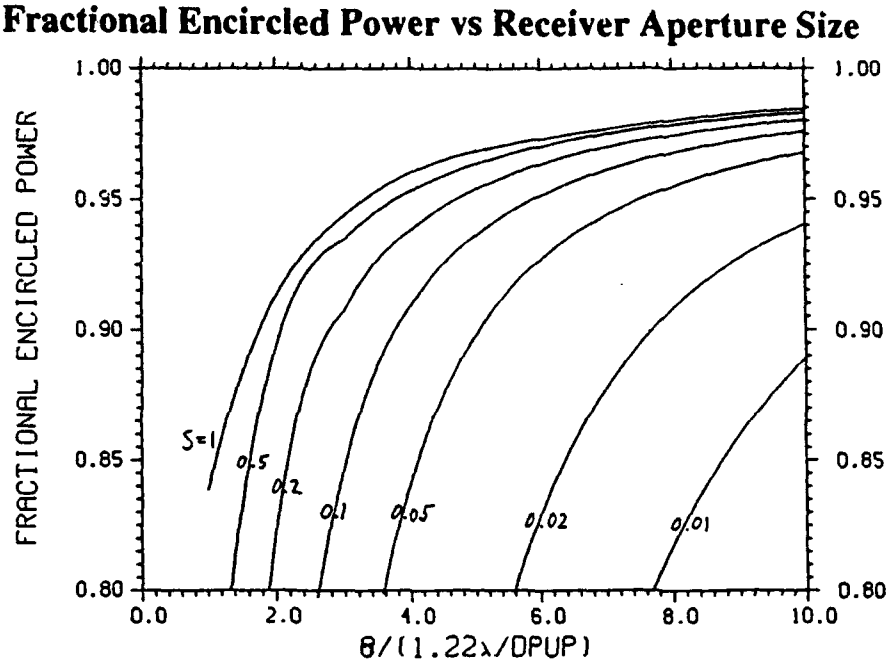

Fig. 2. Fractional Encircled power vs aperture size for several strehls. θ = angular radius of the aperture, λ =0.612μm, D_{pup}= transmitter diameter (10cm). It is seen from the S = 0.05 curve that using a 40 cm diameter receiving aperture will allow detection of over 95% of the incident energy and thus an accurate measurement of the Strehl down to 0.05.

4. EXPERIMENTAL CONDITIONS

A data run consists of a series of 110 images (55 signal and 55 background) taken at half second intervals. Each data run of compensated images was immediately followed by a set of uncompensated images to be used for comparison. Most data runs were taken during early to mid-morning hours from October 6-16, 1992. The path chosen is approximately 3.2 km in length and located about 200 feet above level desert ground. The signal transmitter is located at a telescope site at the Starfire Optical Range and the receiver is located at a small hillside site east of the SOR. Weather conditions were monitored during experiment operation: air temperature, wind speed and direction. During experiment operation turbulence levels, in general, began low in the early morning, dipped briefly during the quiescent period and then rose steadily until becoming saturated some time in the vicinity of 10:00 AM.

Path integrated values of the log amplitude variance and the log C_n^2 were used to indicate the amount of scintillation present in the signal beam and the level of atmospheric turbulence along the path. The log amplitude variance, σ_χ^2, was calculated from the variance of the intensity of the beacon laser on each of the subapertures of the Wavefront Sensor:

$$\sigma_\chi^2 = VAR\left\{0.5\,Log\left(\frac{I_i}{\bar{I}_i}\right)\right\} \qquad (3)$$

where I_i is the intensity of each subaperture from every frame of data in a particular data run and $\bar{I}_i$ is the sample average. σ_χ^2 calculated in this way is averaged over the 7-mm subaperture size and may tend to be slightly smaller than the actual log amplitude variance. Values of σ_χ^2 above 0.3 indicate saturation. The path-average C_n^2 values are calculated from path

integrated r_0 measurements. Scintillation and turbulence conditions measured during the operation of the experiment are shown in Fig. 3. Data points shown in Fig. 3 represent the compilation of all data taken over a number of days. The scatter in these plots is due to the varying weather conditions from day to day. However, the graphs illustrate the general trends of rising scintillation and turbulence from early to mid- morning.

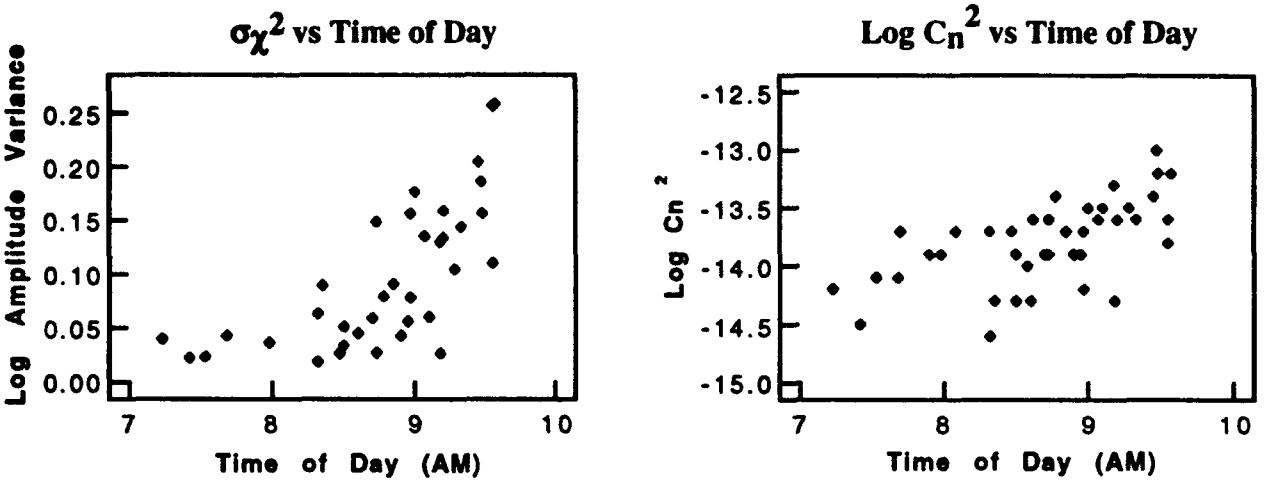

Fig. 3. Scintillation (σ_χ^2) and turbulence conditions (C_n^2) during experiment operation. The atmosphere is shown to become more turbulent until reaching saturated levels by 10 AM.

5. STREHL CALCULATION

Data accumulated over 45 data runs are used to calculate signal Strehls three different ways, as shown in Figs. 4(a) and (b). The long-time-average Strehl (LTavg Strehl) is calculated by averaging the 55 background-subtracted, power normalized, image bearing frames from each data run to produce the time averaged PSF. The Strehl is then calculated from the peak intensity of this time averaged PSF. LT avg Strehl represents the quality of a beam incident on target for a period of about 1 minute.

$$S_{LTavg} = \left[\frac{1}{M} \sum_{k=1}^{M} \frac{I_k(\vec{r})}{P_k} \right]_{max} \cdot \frac{1}{\alpha} . \qquad (4)$$

In Eq. 4, M = the number of frames in a data run, $I_k(\vec{r})$ = the irradiance of the kth background subtracted frame, P_k = power of the kth background-subtracted frame, the quantity in brackets is the maximum of the time-averaged, power-normalized irradiance, and $\alpha = A_p\, g/(\lambda\, z)^2$ (see Eq. 1).

To produce the average single-frame Strehl (SF avg), the peak pixel irradiance of each background-subtracted, power normalized image frame (the quantity in brackets in Eq. 5) is used to calculate individual frame Strehls. The resulting M individual Strehls are then averaged.

$$S_{SFavg} = \frac{1}{M}\sum_{k=1}^{M}\left[\frac{I(\vec{r})}{P_k}\right]_{max} \cdot \frac{1}{\alpha} \qquad (5)$$

The SF avg Strehl indicates the average Strehl of individual frames in each data run and represents the average quality of a 100-μs pulse.

The centroid removed Strehl is, as the name implies, calculated by registering the centroid positions of all image frames from a particular data run before averaging the frames. Each frame is shifted by its centroid position, $\vec{c}_k$, given by

$$\vec{c}_k = \frac{\int \vec{r}\, I_k(\vec{r}) d^2r}{\int I_k(\vec{r}) d^2r} = \int \vec{r}\, \frac{I_k(\vec{r})}{P_k} d^2r \qquad (6)$$

so that the centroids are at a common point before the time-averaged, power normalized irradiance is calculated. This action removes the effect of centroid jitter on the resulting calculation and gives the result expected if the tracking (beam steering) had been perfect. The peak of the centroid removed PSF is then used to calculated the Strehl as in the long-time-average calculation. Thus,

$$S_{Crem} = \frac{1}{M}\sum_{k=1}^{M}\left[\frac{I(\vec{r}+\vec{c}_k)}{P_k}\right]_{max} \cdot \frac{1}{\alpha} \qquad (7)$$

Strehls are calculated for phase compensated and uncompensated data runs and the results are shown in Figs. 4(a) and (b). In each case, the compensated Strehls are higher than uncompensated Strehls indicating that even under highly scintillated conditions phase-only compensation tends to improve the beam quality. There is however a general trend toward decreasing compensated Strehls as the scintillation and turbulence levels increase. A quantity called Strehl Improvement Factor is shown explicitly in Figs. 5(a) and (b). SIF is calculated by dividing the compensated Strehl by its corresponding uncompensated value measured at the same time. SIF vs σ_χ^2 graphs show that the levels of improvement especially in the LT avg case remain fairly constant (at approximately 2 - 4) up to high levels of scintillation. Graphing SIF as a function of C_n^2 shows again that in the measured range of turbulence levels the LT avg improvement is constant. Figure 6 illustrates the improvement in strehl attained by phase only correction by showing a 3-D plot of the irradiance pattern on the receiving aperture for the Centroid removed, the Long-time averaged and the uncorrected cases.

6. EFFECT OF HARDWARE ON STREHL MEASUREMENTS

We examined the calculated Strehl and Strehl improvements under certain hardware bandwidth conditions and coefficient types used in the adaptive optics reconstructor algorithms in order to determine the effect, if any, of the system hardware on the experimental measurements.

Because of hardware limitations, some of the data was taken during periods when the atmospheric Greenwood frequency, f_g, was higher than the operating frequency, f_O. We segregated the data by the magnitude of the ratio of the operating frequency to the atmospheric Greenwood frequency, f_O/f_g. If $f_O/f_g > 1$ then the phase conjugating equipment was operating faster than the atmosphere was changing when that data was taken. If $f_O/f_g < 1$ then the adaptive optics correction loop was slower than atmospheric changes. Although we found a general decrease in Strehl for points having $f_O/f_g < 1$, these points are also associated with higher levels of turbulence and scintillation, which probably accounts for most of the Strehl loss. However, Fig. 7 shows that the Strehl improvement factor tends to increase weakly as the frequency ratio increases indicating that better performance is attained when experiment was performed within the system bandwidth.

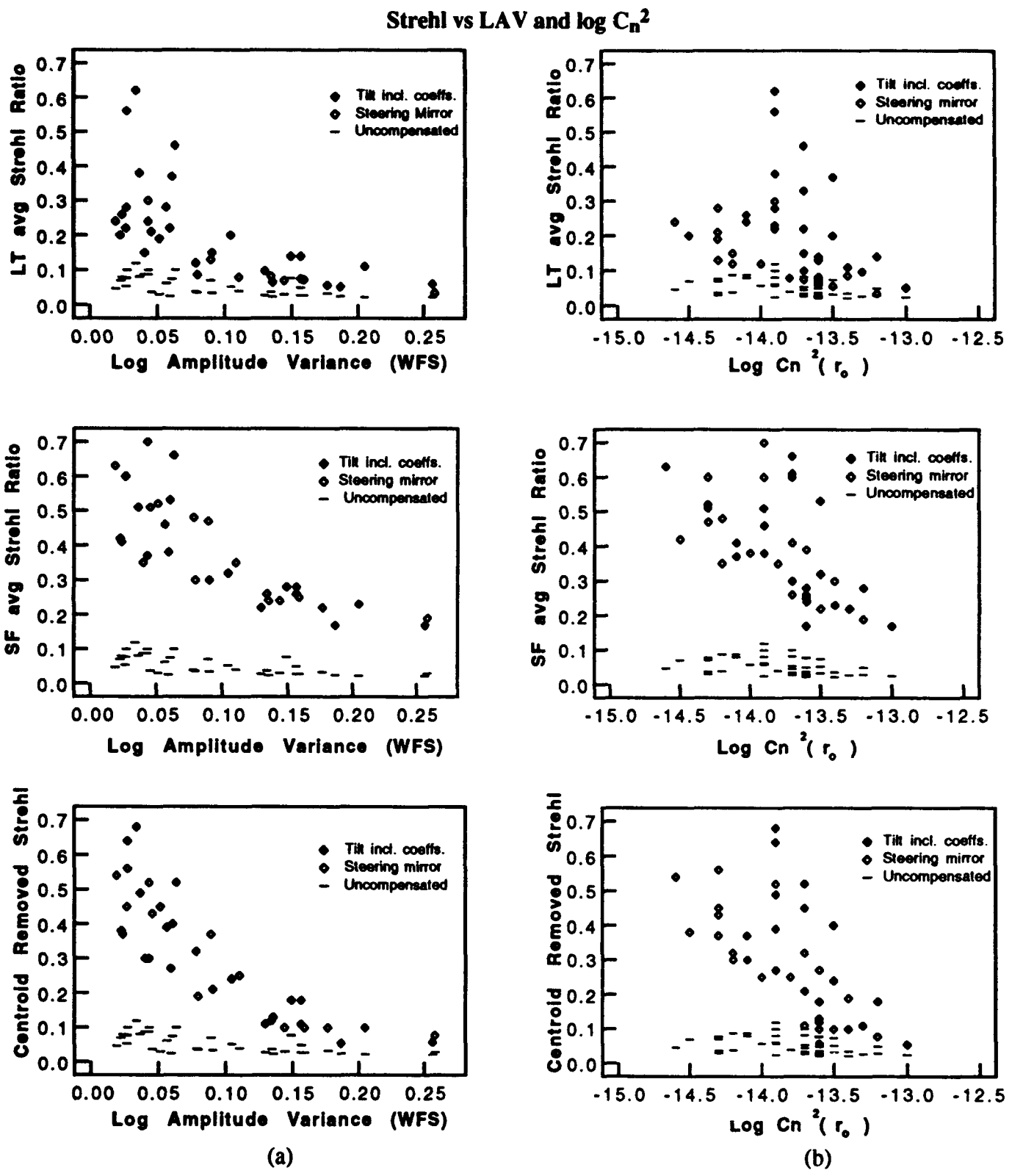

Fig. 4. Long-time average (LT avg), single-frame average (SF avg) and centroid removed Strehls vs (a) log amplitude variance and (b) path integrated log C_n^2.

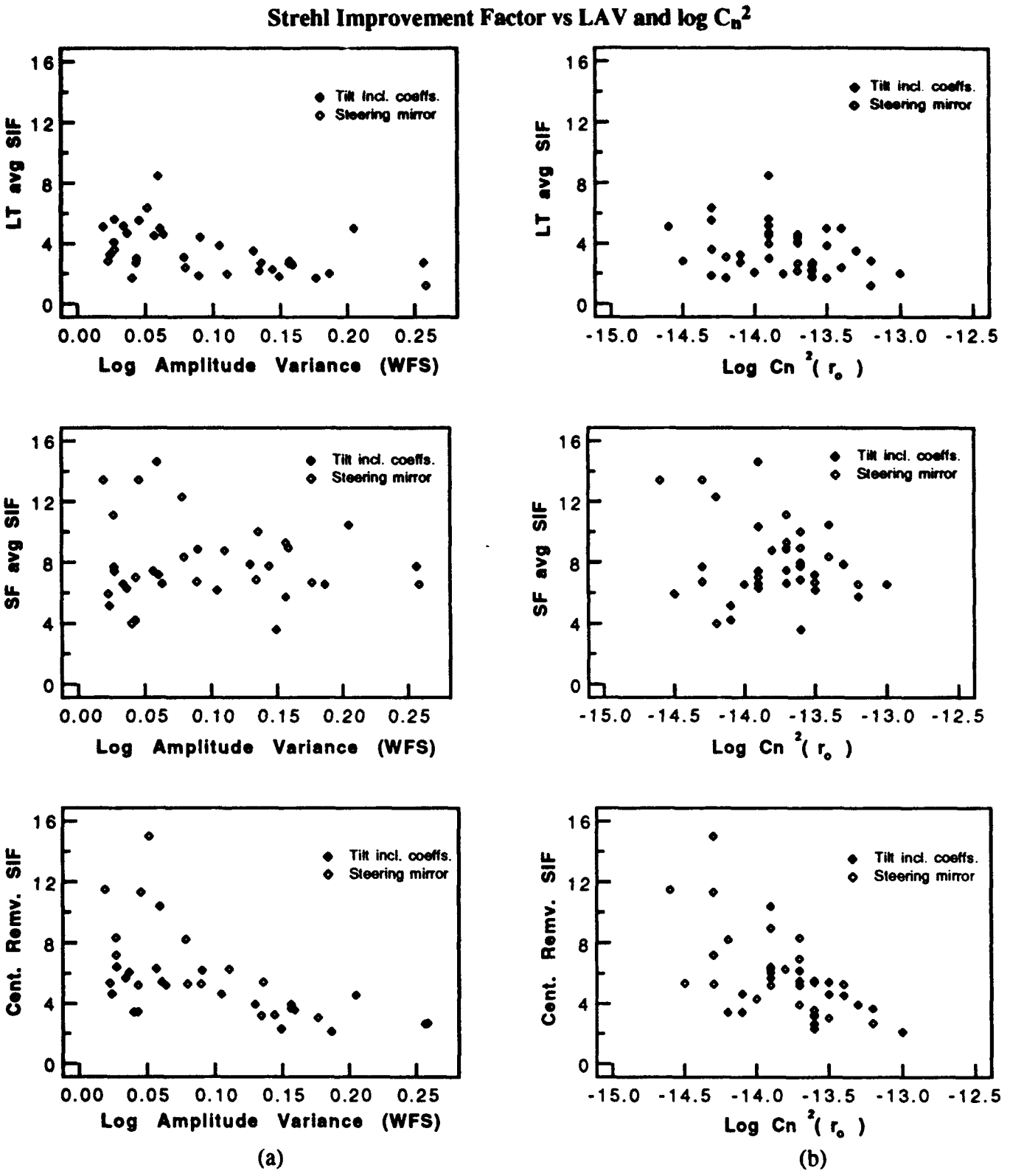

Fig. 5. Long-time average (LT avg), single-frame average (SF avg) and centroid removed Strehl Improvement Factor (SIF) vs (a) log amplitude variance and (b) path-averaged log C_n^2. SIF is the multiplicative factor by which the Strehl is improved by phase compensation.

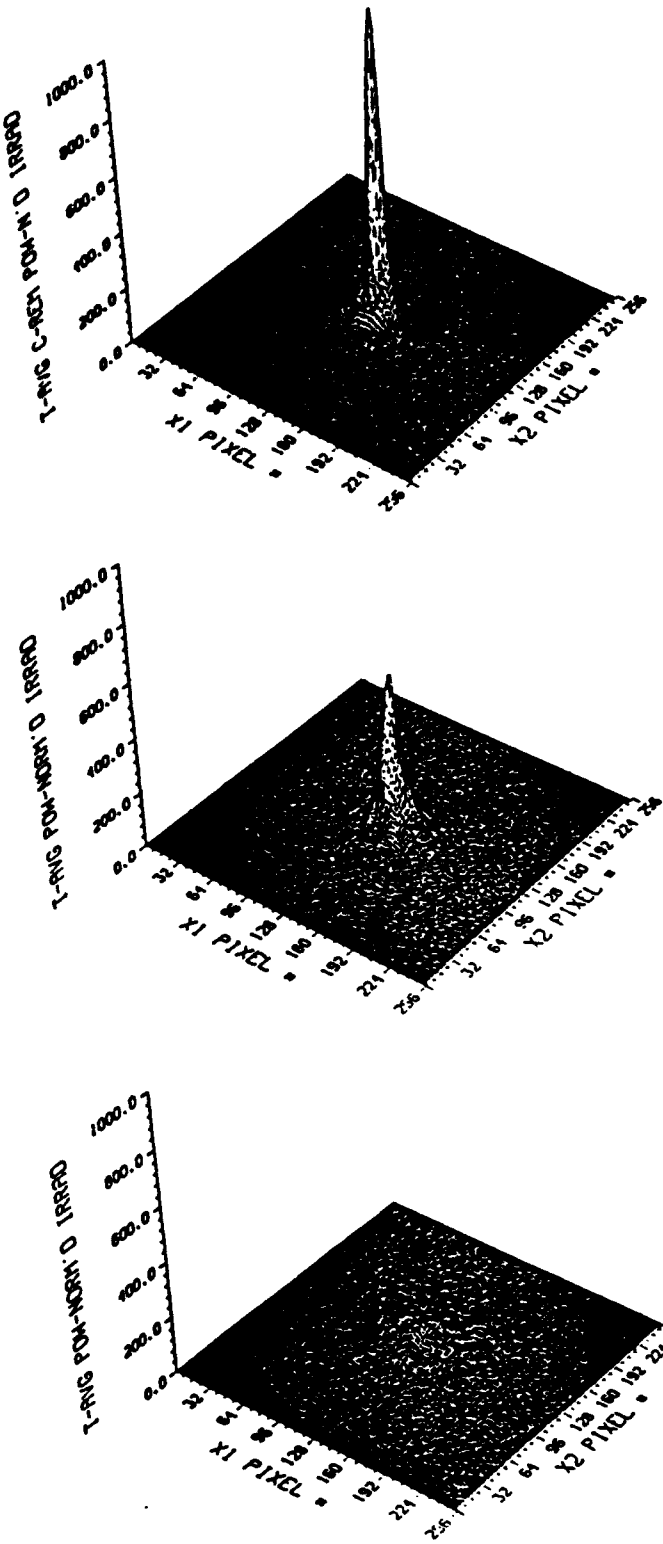

Fig. 6. Plots of receiving aperture PSF's, calculated from a data run taken on October 8, 1992, illustrating the improvement in Strehl when phase correction is used. For cases (a) Centroid Removed, S = 0.43, (b) Long-time Averaged, S = 0.21, and (c) uncorrected, S= 0.038.

Returning to Fig. 4, the data is segregated by the kind of wavefront sensor coefficients used in the reconstructor algorithm. In one case (indicated by Steering Mirror), a steering mirror is used to remove gross tilt from the wavefront before the signal arrives at the adaptive optics. In the other case, the deformable mirror is used to correct for the gross tilt as well as higher order aberrations using tilt-included reconstructor coefficients. Figure 8 indicates that the jitter measured in the centroid position is independent of the frequency ratio but strongly dependent on the WFS coefficients. It is clear from Fig. 8 that the steering-mirror-deformable-mirror combination does not remove as much atmosphere-induced jitter in the measured images as does the deformable mirror alone. We emphasize that this result does not represent an intrinsic limitation of steering mirrors in this application; only that in our case the steering mirror may have been incorrectly stabilized. Jitter tends to reduce the long-time average Strehl and Strehl improvement factor (see Fig. 7). However, jitter does not affect the single-frame average Strehl or the centroid removed Strehl.

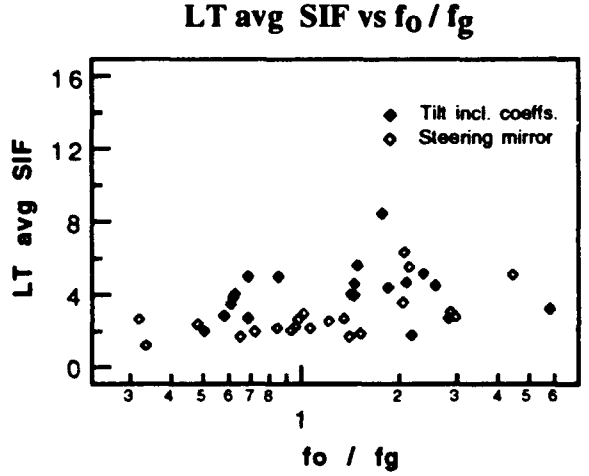

Fig. 7. Long-time average Strehl Improvement factor increases with f_o/f_g. Short -time-average and centroid removed Strehl Improvement factors follow the same trend.

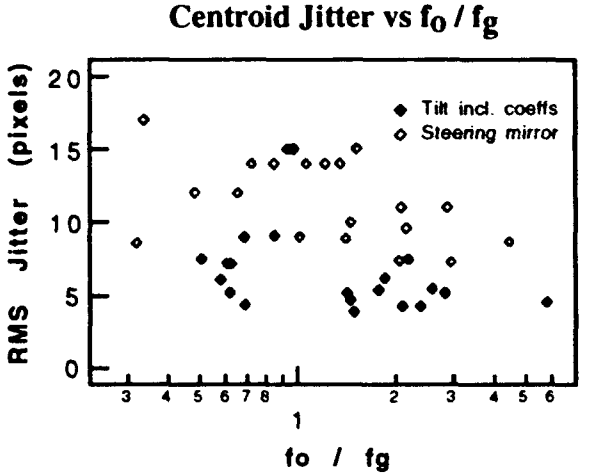

Fig. 8. RMS jitter in the centroid position of the recorded laser beam images vs f_o/f_g. Jitter is not a function of the frequency ratio. Jitter is clearly dependent on whether the steering mirror or tilt included WFS coefficients were used to remove gross tilt in the wavefront.

7. CONCLUSION

We have presented experimental results concerning the effectiveness of phase-only correction of scintillated laser beams. It is shown that phase-only correction improves the beam quality (as measured by the Strehl ratio) even in the presence of strong intensity fluctuations caused by atmospheric turbulence. Although the transmitted beam quality tends to decrease with increasing turbulence and scintillation, the factor by which the adaptive optics improves the Strehl remains fairly constant (by a factor of approximately 2 - 4 times) over the range of turbulence and scintillation conditions tested. We also investigated the effect of the operating bandwidth of the adaptive optics system and the coefficients used in the wavefront sensor algorithm on the resulting strehl measurements. Because most data taken at insufficient operation bandwidth was also associated with high turbulence and scintillation, we found it difficult to separate the effect of bandwidth on Strehl from the effect of the atmosphere. However, it was clearly shown that removing gross tilt in the wavefront with a steering mirror in addition to the deformable mirror was not as effective in removing atmosphere-induced jitter in our experiment as is the use of the deformable mirror alone.